ELSEVIER

Composites Science and Technology 61 (2001) 1821–1832

COMPOSITES SCIENCE AND TECHNOLOGY

www.elsevier.com/locate/compscitech

A new strength model for application of a physically based failure criterion to orthogonal 3D fiber reinforced plastics

J. Juhasz, R. Rolfes, K. Rohwer*

DLR, Institute of Structural Mechanics, PO Box 3267, D-38022 Braunschweig, Germany

Received 12 December 2000; received in revised form 5 May 2001; accepted 7 June 2001

Abstract

A strength model for 3D fiber-reinforced plastics consisting of unidirectional layers with a high in-plane fiber density and additional reinforcements perpendicular to the layers with a significantly lower fiber density is presented. The strength model aims to enhance the application range of an existing, physically based failure criterion for inter-fiber fracture of unidirectional fiber-reinforced layers to the above mentioned configuration of 3D-composites. In doing so the fundamental physical basis, the fracture hypothesis of Mohr, and the general mathematical formulation of the criterion are sustained. The enhancement of the application range is achieved by employing a continuous interpolation between the basic strengths of an orthogonal 3D fiber-reinforced layer. © 2001 Published by Elsevier Science Ltd. All rights reserved.

Keywords: A. Polymer-matrix composites; A. Textile composites; B. Mechanical properties; B. Strength; C. Failure criterion

1. Introduction

One of the most challenging problems in the analysis of the anisotropic mechanical properties of unidirectional fiber-reinforced composites has been the development of adequate failure criteria. Amongst all existing criteria such with macromechanical-phenomenological character, applied to single unidirectional composite layers and using macroscopical stresses and average strengths of these homogenized anisotropic layers are suitable for practical applications. Such criteria exhibit reasonable computational effort, easy determination of material parameters and applicability for design purposes as well as for damage progression analyses. Further on, experimental experiences allow for the following hypothesis:

H1: A fiber reinforced composite layer has different failure modes: fiber fracture (FF) and inter fiber fracture (IFF). FF and IFF are of different nature and require, therefore, different failure criteria [1].

For FF a solution is relatively simple. Experimental results show that FF occurs as primary failure mode of a defect-free composite layer only for normal loads in directions very close to the fiber direction (within approximately 2°). This suggests the following simple max-stress criterion for FF:

$$\left|\frac{\sigma_{||}}{R_{||}^{(+,-)}}\right| = 1, \tag{1}$$

where $\sigma_{||}$ is the stress and $R_{||}^{(+,-)}$ are the strengths of the unidirectional layer for tensile (+) and compressive (−) loads in fiber direction. Puck [2] discussed that more sophisticated models which include the influence of shear and transverse normal stresses on FF lead to deviations less than 5%. Therefore, the simplest model should be used. Eq. (1) is valid for composites where the strain to failure of the fibers is less than that of the matrix. Only in this case FF occurs before IFF and the fiber strength dominates the strength of the layer for normal loads in the fiber direction.

2. Mohr's fracture hypothesis for brittle materials as physical base for IFF of unidirectional composite layers

Failure of the matrix material of fiber reinforced plastics can be looked upon as brittle. Thus a valid

* Corresponding author. Tel.: +49-531-295-2384; fax: +49-531-295-2875.

E-mail address: klaus.rohwer@dlr.de (K. Rohwer).

PII: S0266-3538(01)00083-5

physical base for IFF is Mohr's fracture hypothesis for brittle materials [3]:

H2: The fracture limit of a brittle material is governed by the stresses in the fracture plane.

Hashin [1] postulated the idea to adapt Mohr's fracture plane concept to IFF of unidirectional composite layers. He established the following hypotheses:

H3: IFF always occurs on a plane parallel to the fibers. On such planes no fiber fracture occurs.

H4: If a fiber parallel fracture plane under a fracture angle θ can be identified, IFF will be caused by the interaction of the normal stress σ_N and the shear stresses τ_{NT} and τ_{NL} in the fracture plane (Fig. 1). Therefore an IFF-criterion should be formulated in stresses and strengths of the fracture plane.

Hashin's idea has been taken up by Puck. Based on his experimental experience he established the following additional hypotheses which refine Hashin's original approach:

H5: If $\sigma_N \geqslant 0$, then IFF will be caused by the simultaneously acting transverse tensile stress σ_N and the transverse shear stresses τ_{NT} and τ_{NL}.

H6: If $\sigma_N < 0$, then the transverse compressive stress σ_N generates an additional resistance against the fracture caused by the transverse shear stresses τ_{NT} and τ_{NL}.

Puck [2] developed a mathematical model of a fracture body taking H2 to H6 into account and established the first failure criterion for IFF of unidirectional composite layers with brittle matrix material based on Mohr's fracture hypothesis, the parabolic criterion of Puck (PCP).

On the basis of a work by Jeltsch-Fricker [4], Cuntze et al. [5] studied a number of fracture bodies based on Mohr's fracture hypothesis, including the PCP. The different models were examined in consideration of numerical stability, flexibility for data fitting, experimental effort for determining material parameters and ease of application. Cuntze et al. recommended the so called simple parabolic criterion (SPC). In comparison to the PCP this criterion can be less accurate regarding the data fitting of experimental results, but it offers increased numerical stability and ease of application. The following derivation will use the SPC as a starting point.

3. Mathematical formulation of the SPC for IFF of unidirectional composite layers

Basically the surface of a fracture body in the 6-dimensional stress space can be described by the following Eq. [5]:

$$F(\sigma) = 1 \tag{2}$$

where σ is the stress tensor. Values $F(\sigma) \geqslant 1$ indicate failure. A positive factor $f_R(\sigma)$ can be defined by which a stress state has to be multiplied to make the left-hand side of Eq. (2) equal to 1:

$$F(f_R(\sigma)\cdot\sigma) = 1 \tag{3}$$

$f_R(\sigma)$ is called reserve factor. If $F(\sigma)$ is homogeneous in σ, then $f_R(\sigma)$ can be calculated as follows:

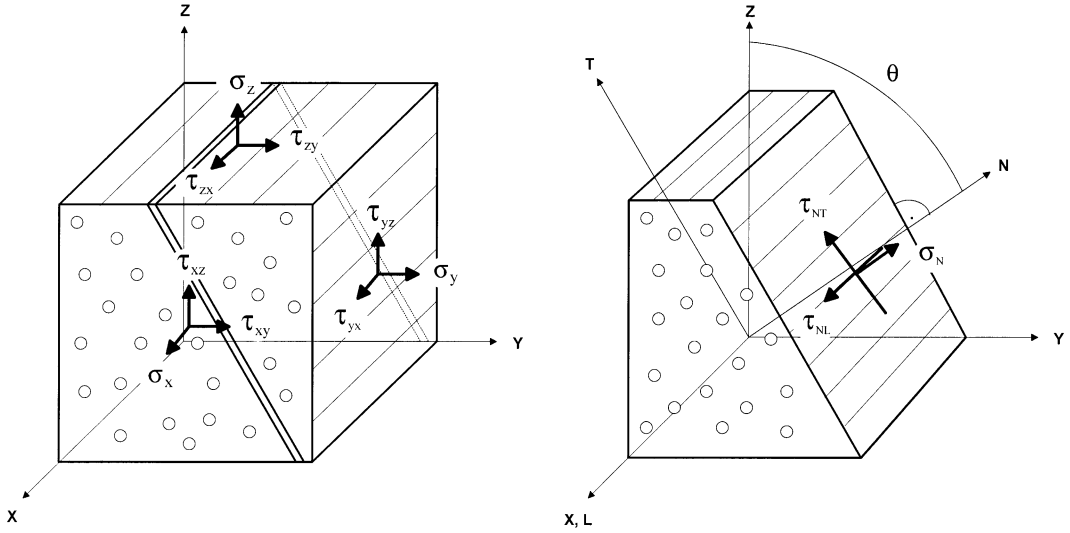

Fig. 1. Components of the stress tensor and stresses in the fracture plane of a unidirectional element.

$$f_R(\sigma) = \frac{1}{\sqrt[k]{F(\sigma)}}, \tag{4}$$

where k is the order of homogeneity. The reserve factor has an infinite value for $\sigma = 0$. Therefore, it is numerically more advantageous to use the reciprocal of $f_R(\sigma)$, the material effort M_E. The well known margin of safety (MoS) is linked to both parameters:

$$\mathrm{MoS} = f_R - 1 = \frac{1}{M_E} - 1 \tag{5}$$

The SPC is represented by the following analytical expressions [5]:

$$\sigma_N \geqslant 0: \sqrt{(1-p^{(+)})^2 \left(\frac{\sigma_N}{R_N^{(+)}}\right)^2 + \left(\frac{\tau_{NT}}{R_{NT}}\right)^2 + \left(\frac{\tau_{NL}}{R_{NL}}\right)^2} + p^{(+)}\frac{\sigma_N}{R_N^{(+)}} = 1 \tag{6}$$

$$\sigma_N < 0: \sqrt{(p^{(-)})^2 \left(\frac{\sigma_N}{R_N^{(-)}}\right)^2 + \left(\frac{\tau_{NT}}{R_{NT}}\right)^2 + \left(\frac{\tau_{NL}}{R_{NL}}\right)^2} + p^{(-)}\frac{\sigma_N}{R_N^{(-)}} = 1 \tag{7}$$

The criterion is formulated solely in stresses and strengths of the fracture plane and forms an ellipsoid for $\sigma_N \geqslant 0$ (presumed $0 < p^{(+)} < 0.5$) and a paraboloid for $\sigma_N < 0$. The parameters $p^{(+,-)}$ represent gradients of the fracture body at certain points (explained in detail below). A quadratic-additive interaction between the fracture plane stresses is assumed. There is no physical rationale for this, it is simply the most effective way to match experimental results by curve fitting [1]. The criterion is homogenous of order one in σ. Therefore, presumed that only external loads are applied, the left-hand sides of Eqs. (6) and (7) represent the material effort M_E.

The stress tensor σ in the (x, y, z)-system has to be transformed into the (L, N, T)-system (Fig. 1). Both the (x, y, z)- and the (L, N, T)-system are orthonormal coordinate systems. The axes of the (x, y, z)-system correspond to the material axes of the layer. Axis L of the (L, N, T)-system is equal to the fiber direction x of the layer, N represents the normal direction of the fracture plane and T is orthonormal to L, N. Due to H3 only a rotation of the normal vector of the fracture plane about the fiber axis is necessary to cover all possible orientations of the fracture plane. Hence θ can vary from $0 \leqslant \theta \leqslant \pi$ (Fig. 1). The stresses in the fracture plane can then be calculated by tensor transformation:

$$\sigma_N = \sigma_y \sin^2\theta + \sigma_z \cos^2\theta + \tau_{yz}\sin 2\theta \tag{8}$$

$$\tau_{NT} = \frac{1}{2}(\sigma_y - \sigma_z)\sin 2\theta + \tau_{yz}\cos 2\theta \tag{9}$$

$$\tau_{NL} = -\tau_{xy}\sin\theta - \tau_{xz}\cos\theta \tag{10}$$

Failure will occur at the angle θ_{max} that makes the left-hand side of Eq. (6) or (7) a global maximum. For a general 3D stress state no analytical solutions for extrema of these equations are known, the maximum has to be calculated in a numerical-iterative way.

Cuntze et al. [5] transformed the strengths of a layer into the strengths of the fracture plane as follows:

$$R_N^{(+)} = R_y^{(+)} = R_z^{(+)} \tag{11}$$

$$R_N^{(-)} = R_y^{(-)} = R_z^{(-)} \tag{12}$$

$$R_{NL} = R_{xy} = R_{xz} \tag{13}$$

$$R_{NT} = \frac{R_N^{(-)}}{1 + \sqrt{1 + 2p^{(-)}}} \tag{14}$$

$R_y^{(+)}$, $R_y^{(-)}$, R_{xy} can be determined by means of simple experiments. R_{yz} is not directly measurable [5]. Therefore, R_{NT} has to be calculated from $R_N^{(-)}$ using Eq. (14). Within the SPC the following coupling between the gradient of the fracture body m_{NL} in the (σ_N, τ_{NL})-plane and the gradient m_{NT} in the (σ_N, τ_{NT})-plane is assumed:

$$\frac{m_{NL}^{(+,-)}}{R_{NL}} = \frac{m_{NT}^{(+,-)}}{R_{NT}} \tag{15}$$

The upper index (+,−) points to approaching $\sigma_N = 0$ from positive or negative values, respectively. Eq. (15) increases the numerical stability of the SPC compared to the PCP. Especially a constriction of the fracture body profile for $\sigma_N \to -\infty$, an effect that can not be observed in the real material behavior, is prevented [5]. The gradients are linked to the parameters $p^{(+,-)}$ in the following way:

$$p^{(+,-)} = -\frac{R_N^{(+,-)}}{R_{NL}} m_{NL}^{(+,-)} \tag{16}$$

$$0 < p^{(+)} < \frac{1}{2} \tag{17}$$

The limitation (17) ensures that Eq. (6) forms an ellipsoid for $\sigma_N \geqslant 0$. For both parameters $p^{(+,-)}$ numerical values can be determined by appropriate tests [5].

There may be an influence of σ_x on IFF. Puck [2] suggests to weaken all layer strengths by a factor $f_w(\sigma_x)$ unless

$$\left|\frac{\sigma_x}{R_x^{(+,-)}}\right| < 0.7 \tag{18}$$

Experimental determination of the influence of the fiber parallel stress σ_x on IFF is difficult. In this paper only those stress states will be considered for which Eq. (18) holds.

4. The situation for 3D fiber reinforced plastics

Conventional composite structures consist of unidirectional layers with in-plane fiber reinforcements in layerwise constant orientations. 3D fiber reinforced composites use additional fiber reinforcements in any out-of-plane direction. While such structures offer improved strength in these directions, the in-plane strength of the layer may be decreased significantly due to increased fiber waviness [6]. Therefore, it is not reasonable to use the same fiber density in out-of-plane directions as in the main fiber direction of the layer. Such a design would just be ineffective and would not take full advantage of the high specific fiber strength. In addition, the manufacturing process of out-of-plane fiber reinforcements is technologically expensive. Easiest to manufacture is a 3D composite with fiber reinforcements perpendicular to the layers. Thus a very common configuration of 3D composites will consist of unidirectional layers with high in-plane fiber density and additional reinforcements exactly perpendicular to the layers with a significantly lower fiber density. The failure criterion to be set up will deal with such a configuration.

The prediction of fracture limits as well as fracture angles using the PCP and SPC has been experimentally verified for unidirectional composites for some selected states of combined stresses [2,5]. The PCP and SPC assume unidirectional layers being transversally isotropic, an idealization that is no longer valid for 3D composite layers. Nevertheless, it can be assumed that the fracture hypothesis of Mohr and the additional hypotheses H2 to H6 remain valid—with certain restrictions—even for IFF of 3D reinforced plastics of the type described above. Then the general mathematical concept and formulation of the SPC, which are based on these hypotheses, can be retained. However, some questions arise:

4.1. The variation of the fracture angle

According to H3 IFF only occurs on planes parallel to fibers. For a z-reinforced layer with x being the main fiber direction there exists only one fiber parallel plane: the x–z plane (Fig. 1). Uniaxial off-axis tests with woven fabrics can simulate the behavior of such layers under plane stress conditions in the x–z plane. Such tests are described in Section 4.5. They reveal that, if the fiber density in x-direction is significantly higher than that in z-direction, IFF occurs in planes parallel to x, but not solely in the x–z plane ($\theta = 90°$). Thus θ still has to be varied to cover all possible orientations of the fracture plane for IFF. The possible range of θ will be $2° \leqslant \theta \leqslant 178°$. For $0 \leqslant \theta < 2°$ and $178° < \theta \leqslant 180°$ the failure mode is FF of the vertical reinforcements.

4.2. The strength parameters

It should be kept in mind that the SPC is a mathematical model based on physical hypotheses and experimental experiences. The parameters of this model have to be adapted to the material behavior. This concerns the strengths of the fracture plane $R_N^{(+,-)}$, R_{NL}, R_{NL} and the gradient parameters $p^{(+,-)}$. The basic strengths of a material are linked to these parameters in a determined way. For different kinds of materials the basic strengths will have not only different values, it is possible that these values have to enter into the parameters of the criterion in a different mathematical way. The SPC assumes a very simple strength model for unidirectional fiber reinforced plastics according to Eqs. (11)–(14). This model is not adequate for 3D fiber reinforced plastics for the following reasons:

- Puck [2] discussed that the assumption $R_N^{(+)} = R_y^{(+)} = R_z^{(+)}$ is an idealization and only valid for $R_{NT} > R_N^{(+)}$. Since the purpose of a z-reinforcement is to increase $R_z^{(+,-)}$ and consequently also $R_N^{(+)}$, this can in general not be presumed for 3D reinforced layers.
- For $\theta = 0$ or $\theta = \pi$ (z-direction, see Fig. 1) the PCP and the SPC indicate delamination as failure mode. Puck [2] recommends to use decreased strength values $R_N^{(+,-)}$ for this fracture plane orientation. This implies $R_y^{(+,-)} \neq R_z^{(+,-)}$, which can not be explicitly accounted for in the PCP/SPC due to the assumption of transversal isotropy. The problem becomes even worse if z-reinforcements are used ($R_y^{(+,-)} << R_z^{(+,-)}$).

Hence a new strength model for $R_N^{(+,-)}$, R_{NT} and R_{NL} that allows for different strengths $R_y^{(+,-)}$ and $R_z^{(+,-)}$ has to be developed. Of course the development of such a model must be based on experimental results. Very beneficial and easy to perform experiments are uniaxial off-axis tests under normal loads. Using data points for the IFF-strength for various off-axis angles, normal as well as shear strength values can be determined simultaneously (see Sections 5.2.–5.4). For orthogonal 3D fiber reinforced plastics the strength behavior for plane stresses in the x–y, x–z and y–z plane is of interest. The x–y and y–z plane are planes with fiber reinforcements in one direction, the x–z plane is a plane with fiber reinforcements in two directions.

4.3. IFF-strength for plane stress in the x–y plane

As mentioned above the additional fiber reinforcement in z-direction weakens the fiber dominated

strength in x-direction due to increased fiber ondulation. Therefore the absolute in-plane strength of the layer is decreased. However, the dependency of the IFF strength on the off-axis load angle should remain similar to that of a unidirectional layer. Uniaxial off-axis tension test results for unidirectional composites have been reported e.g. by Hashin and Rotem [7] and are plotted in Fig. 2.

The chart shows the IFF-strength of a unidirectional layer R_{IFF} as function of the angle α between the fiber axis and the load axis as measured by Hashin and Rotem. This angle varies from the x-axis ($\alpha = 0$) to the y-axis ($\alpha = 90°$). For $0 \leqslant \alpha < 2°$ the failure mode is FF, otherwise IFF. According to Fig. 2 the criterion has to model a hyperbolic decrease of R_{IFF} with increasing off-axis angle from $R_{IFF} = R_x^{(+)}$ for $\alpha = 2°$ to $R_{IFF} = R_y^{(+)}$ for $\alpha = 90°$.

4.4. IFF-strength for plane stress in the y–z plane

The off-axis angle α now varies from the z-axis ($\alpha = 0$) to the y-axis ($\alpha = 90°$). For $0 \leqslant \alpha < 2°$ the failure mode is FF, otherwise IFF. The strength behavior is similar to that in the x–y plane. The only difference is a different curve shape due to $R_z^{(+)} < R_x^{(+)}$. The criterion has to model a hyperbolic decrease of R_{IFF} with increasing off-axis angle from $R_{IFF} = R_z^{(+)}$ for $\alpha = 2°$ to $R_{IFF} = R_y^{(+)}$ for $\alpha = 90°$.

4.5. IFF-strength for plane stress in the x–z plane

In this plane the situation is somewhat different because of fiber reinforcements in two directions. The off-axis angle α now varies from the x-axis ($\alpha = 0$) to the z-axis ($\alpha = 90°$). For $0 \leqslant \alpha < 2°$ and $88° < \alpha \leqslant 90°$ the failure mode is FF, otherwise IFF.

The authors have carried out uniaxial tension tests with off-axis specimen to determine the strength behavior between two fiber dominated strengths $R_x^{(+)}$ and $R_z^{(+)}$ of a layer. Using woven fabrics with different fiber densities in fill and warp direction is a simple and effective way to manufacture such specimens. The fill direction with the higher fiber density then represents the x-direction of the simulated 3D composite, the warp direction is the z-direction.

One may question the validity of such tests to the present problem because of the relative high fiber ondulation of fabrics. However, real 3D composites exhibit fiber ondulation too. Further on, if a normal tension load is applied, then the fibers are more and more stretched until they are nearly straight. At this point the layer reaches its maximum Young's modulus. Subsequently the modulus decreases slightly due to nonlinear effects until final failure occurs. This effect has actually been observed by the authors in the tests (Fig. 3). Thus the fabric tests can be considered as a good approximation to the case of plane stress in the x–z plane of 3D composites. The test results are plotted in Fig. 4.

The ratio of the strength in fill (x) and warp (z) direction is $R_x^{(+)}/R_z^{(+)} \approx 10$. Assuming that the strength of the layer for loads in the x- and z-direction, respectively, is higher than for loads in directions between these axes, a minimum of R_{IFF} should be observable in the range between $60° < \alpha < 85°$. However, scattering of the test data does not make this very clear (for all data points five

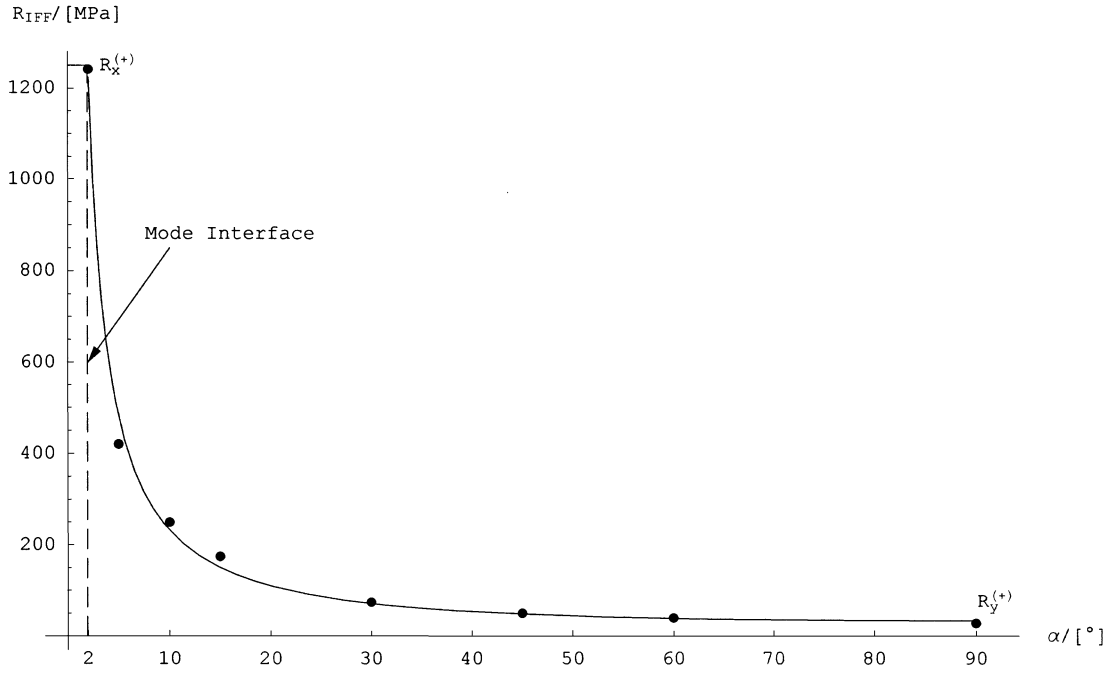

Fig. 2. Test results by Hashin and Rotem [7] for off-axis loads in the x–y plane.

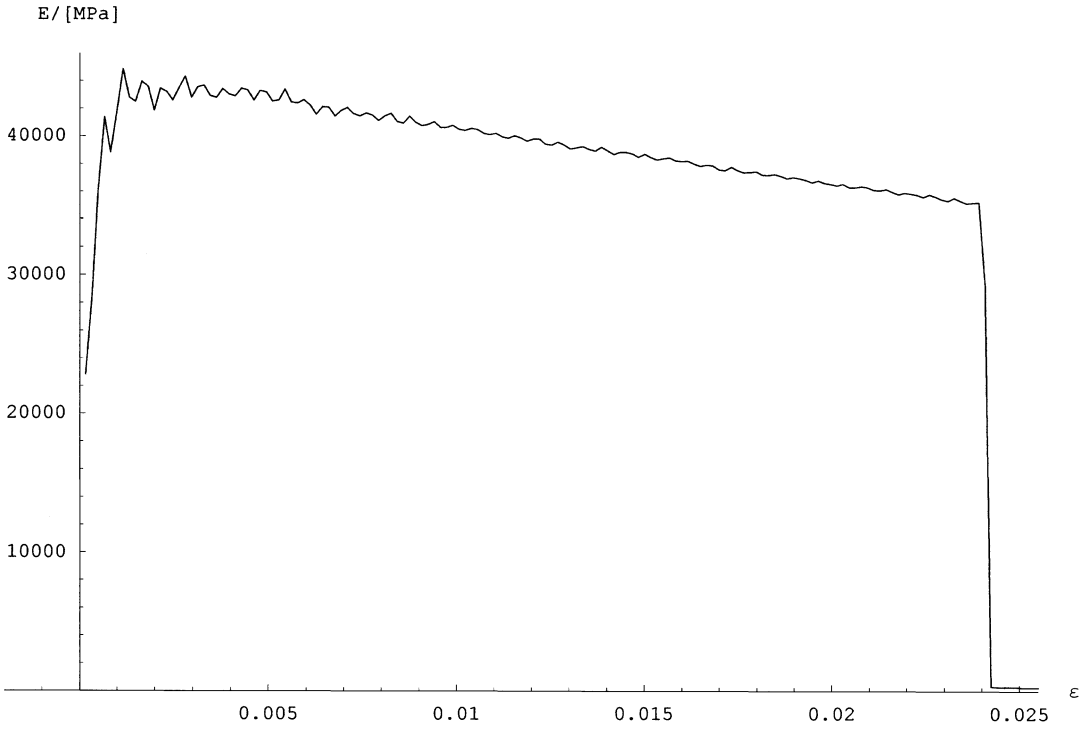

Fig. 3. Young's modulus E over strain ε, experimental results of a woven fabric loaded in fill direction.

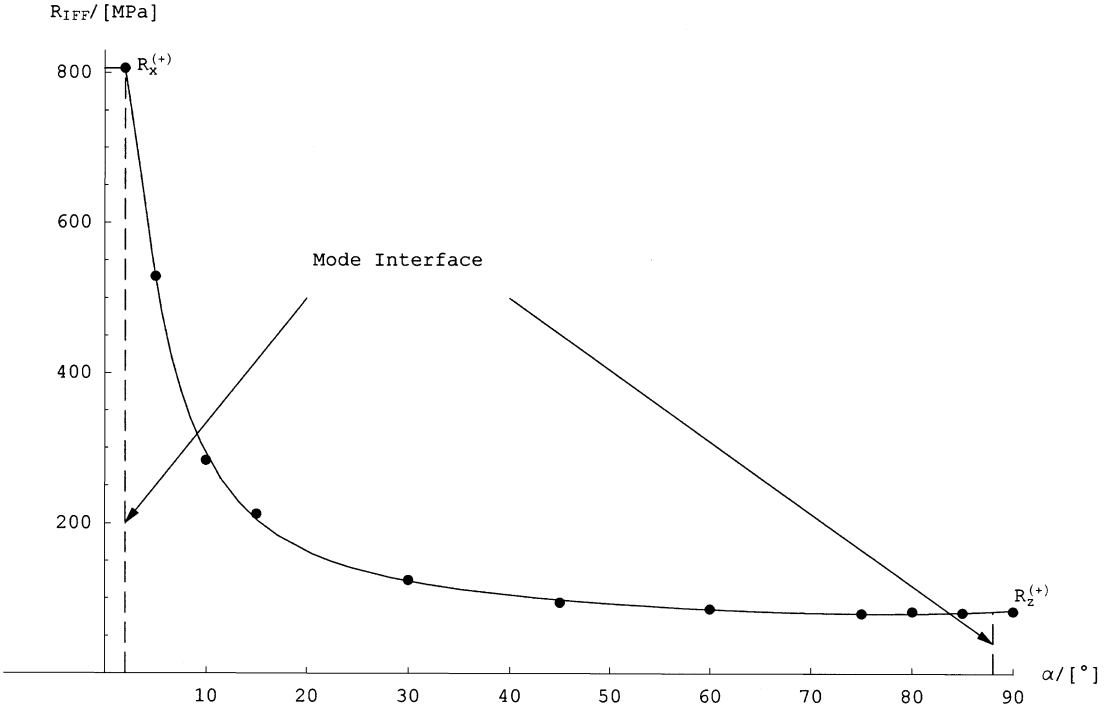

Fig. 4. Test results for off-axis loads in the x–y plane.

measurements were made, at $\alpha = 60$, 75, 80, 85 and 90° the standard deviation was approximately 5 MPa compared to strength values of about 80 MPa). Thus for the here tested configuration the strength behavior is similar to that in the x–y plane. However, that must be different for other strength ratios $R_x^{(+)}/R_z^{(+)}$. For $R_x^{(+)} = R_z^{(+)}$ for instance, R_{IFF} must be minimal at $\alpha = 45°$ and maximal at $\alpha = 2°$ and $\alpha = 88°$ obviously.

Therefore, for $R_x^{(+)} \geqslant R_z^{(+)}$ it is assumed that the criterion should describe a parabolic strength behavior of R_{IFF}

varying from $R_{IFF} = R_x^{(+)}$ at $\alpha = 2^\circ$ to $R_{IFF} = R_z^{(+)}$ at $\alpha = 88^\circ$ with a minimum of R_{IFF} between $45^\circ \leqslant \alpha_{min} \leqslant 88^\circ$.

4.6. Compression strength

How exactly an orthogonal 3D fiber reinforced plastic behaves under plane uniaxial off-axis compression loads in the x–y, x–z and y–z planes must be determined by appropriate tests. Until such tests are performed a similar behavior as for tension loads is supposed with the substitutions $R_x^{(+)} \rightarrow R_x^{(-)}$, $R_y^{(+)} \rightarrow R_y^{(-)}$ and $R_z^{(+)} \rightarrow R_z^{(-)}$. For the fiber dominated strengths in x- and z-direction $R_x^{(-)} \approx R_x^{(+)}$ and $R_z^{(-)} \approx R_z^{(+)}$ are assumed, while for the matrix dominated strength in y-direction $R_y^{(+)} < R_y^{(-)}$ should hold.

5. Adaptation of the SPC to IFF of orthogonal 3D fiber reinforced plastics

The question is now how the basic strengths of the layer $R_x^{(+,-)}$, $R_y^{(+,-)}$, $R_z^{(+,-)}$, R_{xy}, R_{xz} and R_{yz} should be connected to the strengths $R_N^{(+,-)}$, R_{NT} and R_{NL} of the fracture plane to achieve the required behavior of R_{IFF}. In expressions (8)–(10) the stresses in the fracture plane are obtained by tensor transformation. It can be observed that the normal stresses σ_y, σ_z and the shear stress τ_{yz} have an influence on σ_N. Hence the strength R_N should not only depend on the values of R_y and R_z, but also on the shear strength R_{yz}. Similarly R_{NT} should take into account R_{yz} as well as R_y and R_z. Only R_{NL} must depend on the shear strengths R_{xy} and R_{xz} alone.

According to Eqs (8)–(10) the particular strength values should enter into the criterion in a similar way as the stresses do. It is realistic that a basic strength of the layer contributes to a strength of the fracture plane in dependence of the fracture angle. However, while stresses can interact with each other (see H5 and H6), the sign dependence due to the trigonometric functions has to be eliminated for the strength transformation. One strength value can not influence another one. As a possible solution to model this behavior the following strength model is proposed:

$$R_N^{(+,-)} = \tilde{R}_y^{(+,-)} \sin^2\theta + \tilde{R}_z^{(+,-)} \cos^2\theta + \tilde{R}_{yz} \,|\sin 2\theta| \tag{19}$$

$$R_{NL} = \tilde{R}_{xy} \,|\sin\theta| + \tilde{R}_{xz} \,|\cos\theta| \tag{20}$$

$$R_{NT}^{(+,-)} = \frac{1}{2}(\tilde{R}_y^{(+,-)} + \tilde{R}_z^{(+,-)}) \cdot |\sin 2\theta| + \tilde{R}_{yz} \tag{21}$$

5.1. Discussion of the new strength model

1. It is important to mention that in general the strength parameters $\tilde{R}_y^{(+,-)}$, $\tilde{R}_z^{(+,-)}$, $\tilde{R}_{xy}$, $\tilde{R}_{xz}$, $\tilde{R}_{yz}$ used in Eqs (19)–(21) are not equal to the basic strengths of the layer $R_y^{(+,-)}$, $R_z^{(+,-)}$, R_{xy}, R_{xz}, R_{yz}. They are parameters of a mathematical model which are adapted to experimental results.

2. The fiber dominated strength $R_x^{(+,-)}$ has no direct influence. However, this strength is a boundary condition in the fitting process for the strength parameters (see Sections 5.2–5.4).

3. $R_N^{(+,-)}$ varies between $\tilde{R}_z^{(+,-)}$ at $\theta = 0^\circ$, $\theta = 180^\circ$ and $\tilde{R}_y^{(+,-)}$ at $\theta = 90^\circ$ in the same way as σ_N does between σ_z and σ_y in Eq. (8). At other angles an offset for additional resistance against τ_{yz} is added.

4. R_{NL} is only slightly modulated between $\tilde{R}_{xz}$ at $\theta = 0^\circ$, $\theta = 180^\circ$ and $\tilde{R}_{xy}$ at $\theta = 90^\circ$.

5. $R_{NT}^{(+,-)}$ is directly related to $\tilde{R}_{yz}$. At angles $\theta \neq 0^\circ$, $\theta \neq 90^\circ$, $\theta \neq 180^\circ$ an average value of $\tilde{R}_y^{(+,-)}$ and $\tilde{R}_z^{(+,-)}$ is added in dependence on $|\sin 2\theta|$. $R_{NT}^{(+,-)}$ is now different for $\sigma_N \geqslant 0$ and $\sigma_N < 0$. Thus the SPC must be modified to yield:

$$\sigma_N \geqslant 0 : \sqrt{(1 - p^{(+)})^2 \left(\frac{\sigma_N}{R_N^{(+)}}\right)^2 + \left(\frac{\tau_{NT}}{R_{NT}^{(+)}}\right)^2 + \left(\frac{\tau_{NL}}{R_{NL}}\right)^2} + p^{(+)} \frac{\sigma_N}{R_N^{(+)}} = 1 \tag{22}$$

$$\sigma_N < 0 : \sqrt{(p^{(-)})^2 \left(\frac{\sigma_N}{R_N^{(-)}}\right)^2 + \left(\frac{\tau_{NT}}{R_{NT}^{(-)}}\right)^2 + \left(\frac{\tau_{NL}}{R_{NL}}\right)^2} + p^{(-)} \frac{\sigma_N}{R_N^{(-)}} = 1 \tag{23}$$

Figs. 5 and 6 show the resulting curves of the fracture plane strengths for characteristic CFRP strength parameters listed in Table 1.

In the following the failure prediction of the SPC for plane off-axis loads in the x–y, x–z and y–z planes is compared with the required behavior for R_{IFF} as discussed in Section 4.

The basic strengths $R_x^{(+)}$ and $R_y^{(+)}$ measured by Hashin and Rotem [7] are used to allow for a direct comparison (Fig. 2). The test results measured by the authors (Fig. 4) do not correspond to these values since a different material was used. In order to obtain a complete data set, exemplary strength values $R_z^{(+,-)}$ are assumed. Table 1 shows these values as well as the strength parameters used in the SPC. The latter are determined by means of a fitting process as described below.

5.2. Failure prediction for off-axis loads in the x–y plane

An off-axis load σ_{oa} in the x–y plane can be split up into the components with respect to the material axes as follows (off-axis angle α, see Section 4):

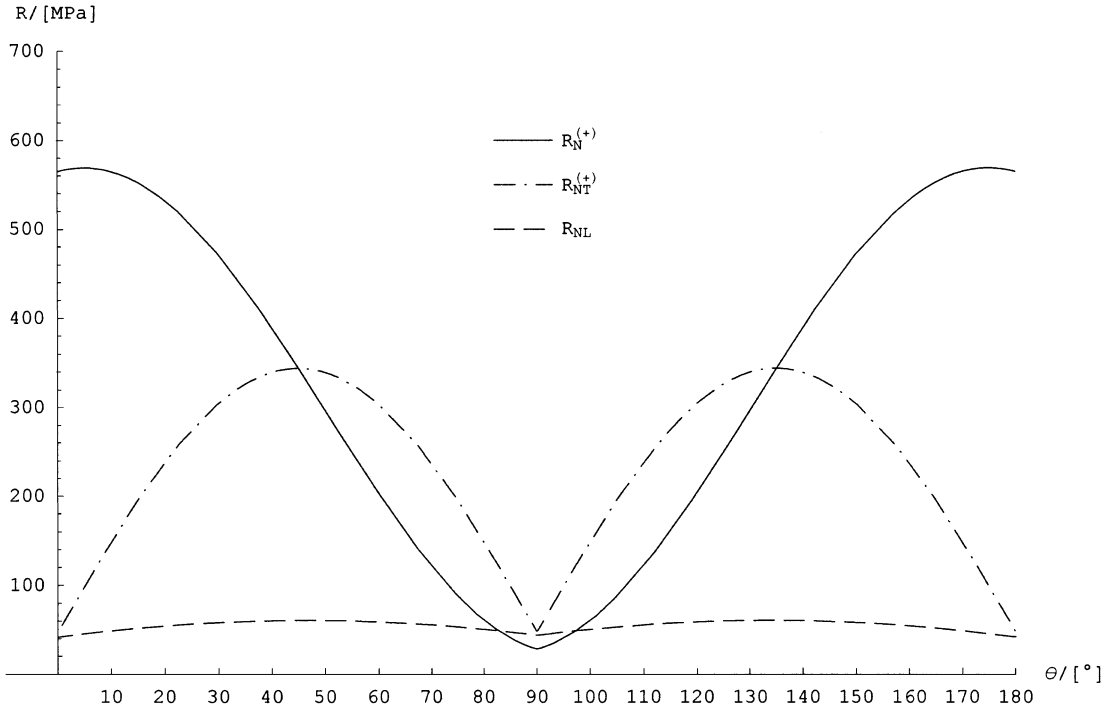

Fig. 5. Fracture plane strengths $R_N^{(+)}$, $R_{NT}^{(+)}$, R_{NL} for $\sigma_N \geqslant 0$.

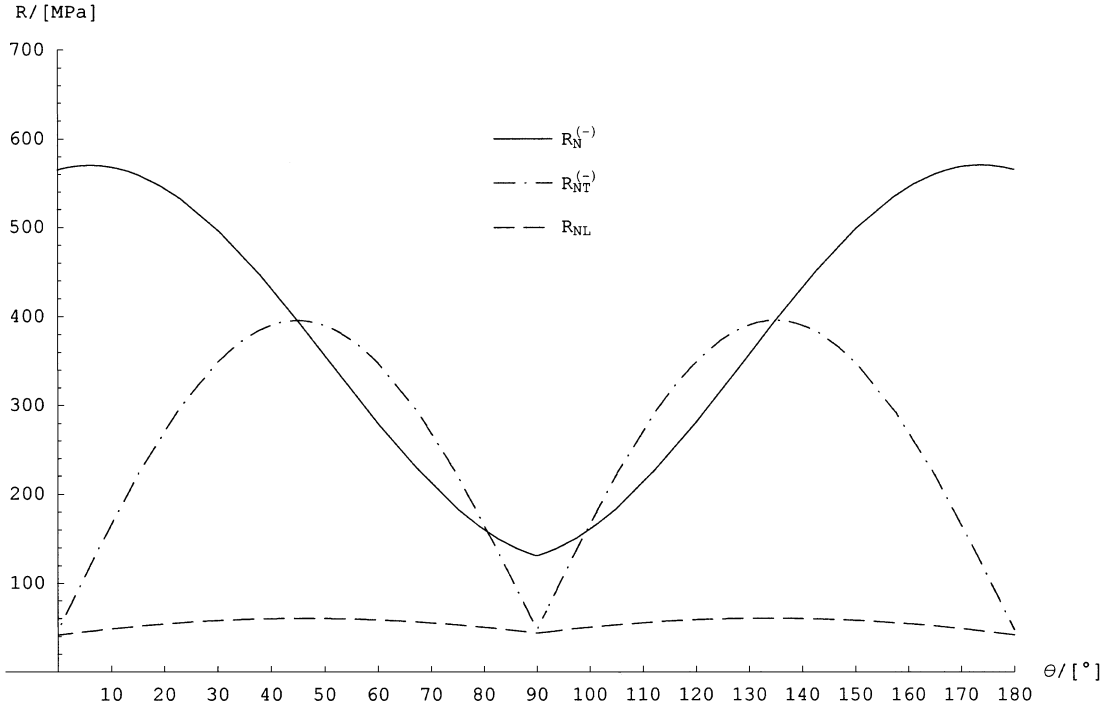

Fig. 6. Fracture plane strengths $R_N^{(-)}$, $R_{NT}^{(-)}$, R_{NL} for $\sigma_N < 0$.

$$\sigma_x = \sigma_{oa}\cos^2\alpha \tag{24}$$

$$\sigma_y = \sigma_{oa}\sin^2\alpha \tag{25}$$

$$\tau_{xy} = \sigma_{oa}\sin\alpha\cdot\cos\alpha \tag{26}$$

For one selected off-axis angle α it is now possible to insert these expressions into Eqs. (8)–(10) to obtain the fracture plane stresses. In a next step Eq. (22) for tension loads $\sigma_{oa} \geqslant 0$ or Eq. (23) for compression loads $\sigma_{oa} < 0$, respectively, can be solved for σ_{oa} varying the

fracture plane angle θ from $2^\circ \leqslant \theta \leqslant 178^\circ$. The minimal value of σ_{oa} in this variation is then equal to the IFF-strength $R_{IFF}^{(+)}$ (tension) and $R_{IFF}^{(-)}$ (compression), respectively. This procedure must be repeated for every off-axis angle α.

Fitting procedure: For a plane stress in the x–y plane the SPC indicates only $\theta = 90^\circ$ as fracture angle. Then, according to Eqs.(19)–(21), only the strengths $\tilde{R}_y^{(+,-)}$ and $\tilde{R}_{xy}$ (besides the gradient parameters $p^{(+,-)}$) have an influence on the predicted failure. They are adapted to data points in this plane. As pointed out by Cuntze et al. [5] the x–y plane is also the preferred plane for determination of the gradient parameters $p^{(+,-)}$. The numerical values can be calculated by standard statistical methods or "manually". Results of such a procedure are listed in Table 1.

Fig. 7 shows the failure in the x–y plane as predicted by the SPC. The criterion yields the required hyperbolic decrease of $R_{IFF}^{(+)}$. The agreement with the test results measured by Hashin and Rotem [7] is good. At higher off-axis angles the theoretical values of $R_{IFF}^{(-)}$ are larger than those of $R_{IFF}^{(+)}$, reflecting hypothesis H6. Whether or not this behavior coincides with reality remains to be checked by off-axis compression tests.

Table 1
Comparison of basic strengths of a layer and strengths parameters used in the SPC

Basic strengths of the layer	Strength and gradient parameters in the SPC
$R_x^{(+)} = 1241$ MPa	
$R_x^{(-)} = 1241$ MPa	
$R_y^{(+)} = 28.3$ MPa	$\tilde{R}_y^{(+)} = 28.3$ MPa
$R_y^{(-)} = 131$ MPa	$\tilde{R}_y^{(-)} = 131$ MPa
$R_z^{(+)} = 500$ MPa	$\tilde{R}_z^{(+)} = 565$ MPa
$R_z^{(-)} = 500$ MPa	$\tilde{R}_z^{(-)} = 565$ MPa
	$\tilde{R}_{xy} = 43.8$ MPa
	$\tilde{R}_{xz} = 41.8$ MPa
	$\tilde{R}_{yz} = 47.5$ MPa
	$p^{(+)} = 0.2$
	$p^{(-)} = -0.5$

5.3. Failure prediction for off-axis loads in the x–z plane

An off-axis load σ_{oa} in the x–z plane can be split up into the components with respect to the material axes as follows:

$$\sigma_x = \sigma_{oa}\cos^2\alpha \tag{27}$$

$$\sigma_z = \sigma_{oa}\sin^2\alpha \tag{28}$$

$$\tau_{xz} = \sigma_{oa}\sin\alpha\cdot\cos\alpha \tag{29}$$

Again the expressions are inserted into Eqs. (8)–(10), then R_{IFF} is calculated in the same way as in the x–y plane.

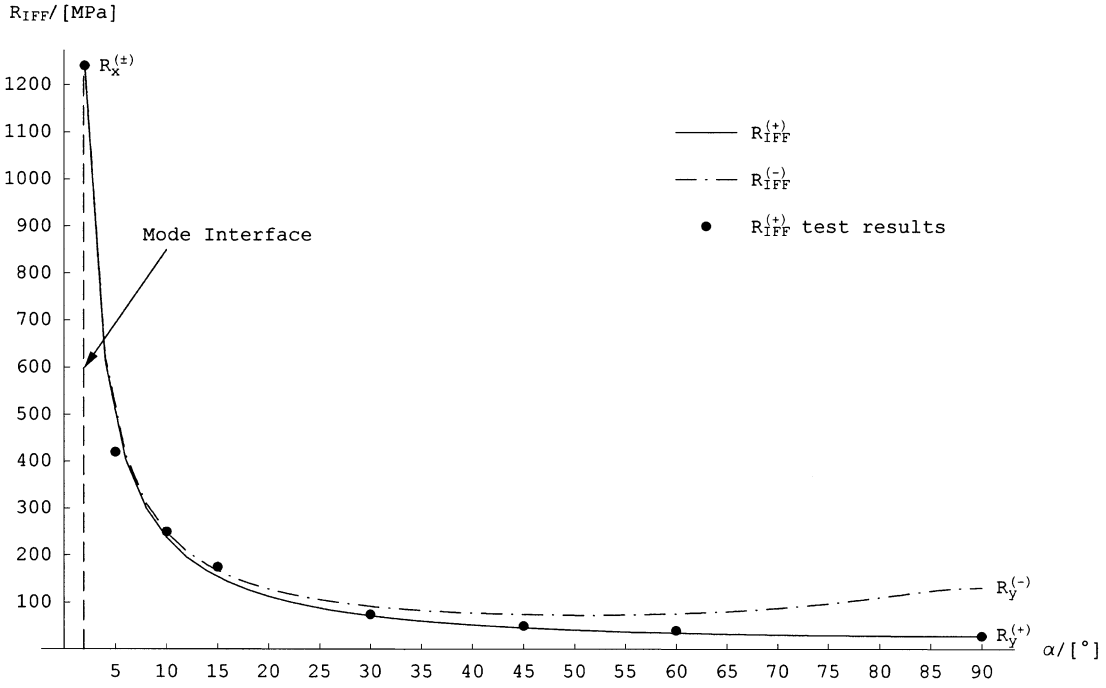

Fig. 7. Failure prediction of the SPC for plane off-axis loads in the *x–y* plane.

Fitting procedure: For a plane stress in the x–z plane the fracture angle θ varies, however, it remains small ($2^\circ \leqslant \theta \leqslant 10^\circ$). Therefore, according to Eqs (19)–(21), mainly the strength parameters $\tilde{R}_z^{(+,-)}$ and $\tilde{R}_{xz}$ have an effect on the predicted failure. $\tilde{R}_{xz}$ can be adapted to data points in the x–z plane alone, while for $\tilde{R}_z^{(+,-)}$ the y–z plane has to be taken into account, too. The gradient parameters $p^{(+,-)}$ offer additional flexibility. In this way the values of $\tilde{R}_z^{(+,-)}$ and $\tilde{R}_{xz}$ listed in Table 1 are calculated.

Fig. 8 shows that the SPC predicts a behavior of R_{IFF} as required. However, whether the curve shape is realistic or not for a strength ratio of $R_x^{(+)}/R_z^{(+)} = 1241\ \text{MPa}/500\ \text{MPa}$ also remains to be shown by appropriate tests.

5.4. Failure prediction for off-axis loads in the y–z plane

An off-axis load σ_{oa} in the y–z plane can be split up into the components in respect to the material axes as follows:

$$\sigma_y = \sigma_{oa}\sin^2\alpha \tag{30}$$

$$\sigma_z = \sigma_{oa}\cos^2\alpha \tag{31}$$

$$\tau_{yz} = \sigma_{oa}\sin\alpha\cdot\cos\alpha \tag{32}$$

These expressions can be inserted into Eqs. (8)–(10). Then the procedure of calculating R_{IFF} is equal to that in the x–y plane.

Fitting procedure: For a plane stress in the y–z plane the fracture angle θ varies. The values for $\tilde{R}_y^{(+,-)}$, $\tilde{R}_{xy}$, $\tilde{R}_{xz}$ should not be modified any more. A value for $\tilde{R}_{yz}$ can be determined finally, the values for $\tilde{R}_z^{(+,-)}$ can be verified. The gradient parameters $p^{(+,-)}$ offer additional flexibility. In this way the value for $\tilde{R}_{yz}$ listed in Table 1 is determined.

Fig. 9 shows that the resulting behavior of $R_{IFF}^{(+)}$ in the y–z plane is again a hyperbolic one, $R_{IFF}^{(-)}$ shows a similar tendency as in the x–y plane (see Fig. 7).

5.5. Summary

It has been demonstrated that the SPC and the strength model according to Eqs (19)–(21) are able to model the strength behavior as requested in Section 4 for off-axis tension loads in the x–y, x–z and y–z planes. Appropriate tests have to be conducted to validate the theoretical predictions for off-axis compression loads.

6. Practical application of the SPC for orthogonal 3D fiber reinforced plastics

6.1. General handling for orthogonal 3D fiber reinforced composites

FF: Eq. (1) must now be applied for both the x- and z-direction with the substitutions $\sigma_{||} \rightarrow \sigma_x$, σ_z and $R_{||}^{(+,-)} \rightarrow R_x^{(+,-)}$, $R_z^{(+,-)}$, respectively.

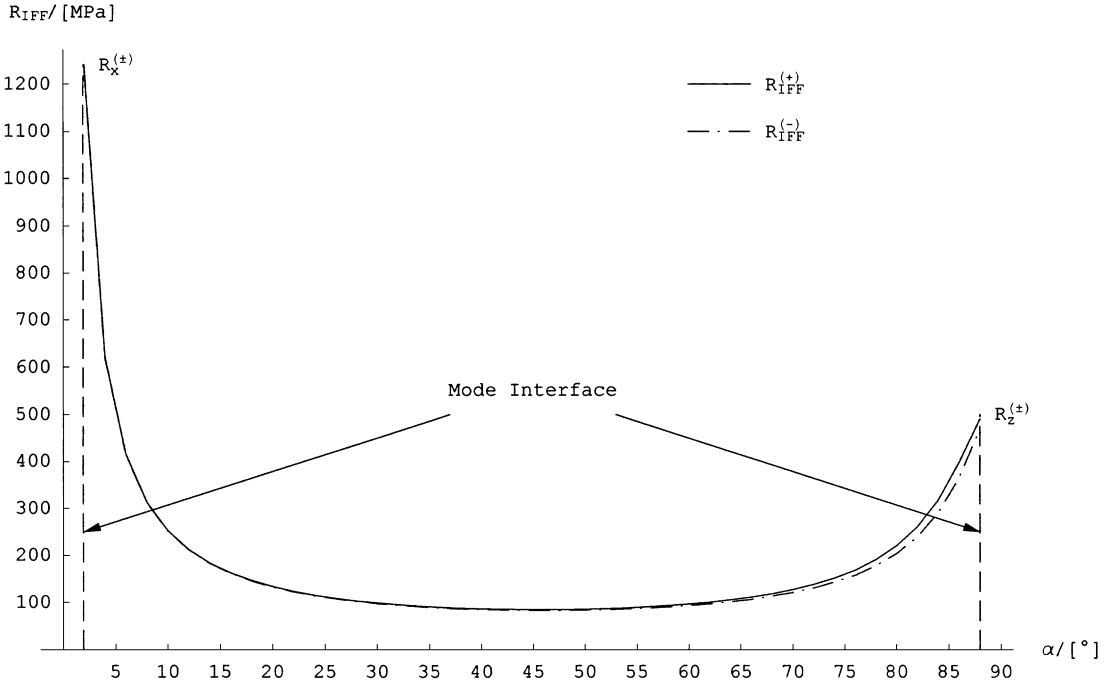

Fig. 8. Failure prediction of the SPC for plane off-axis loads in the x–z plane.

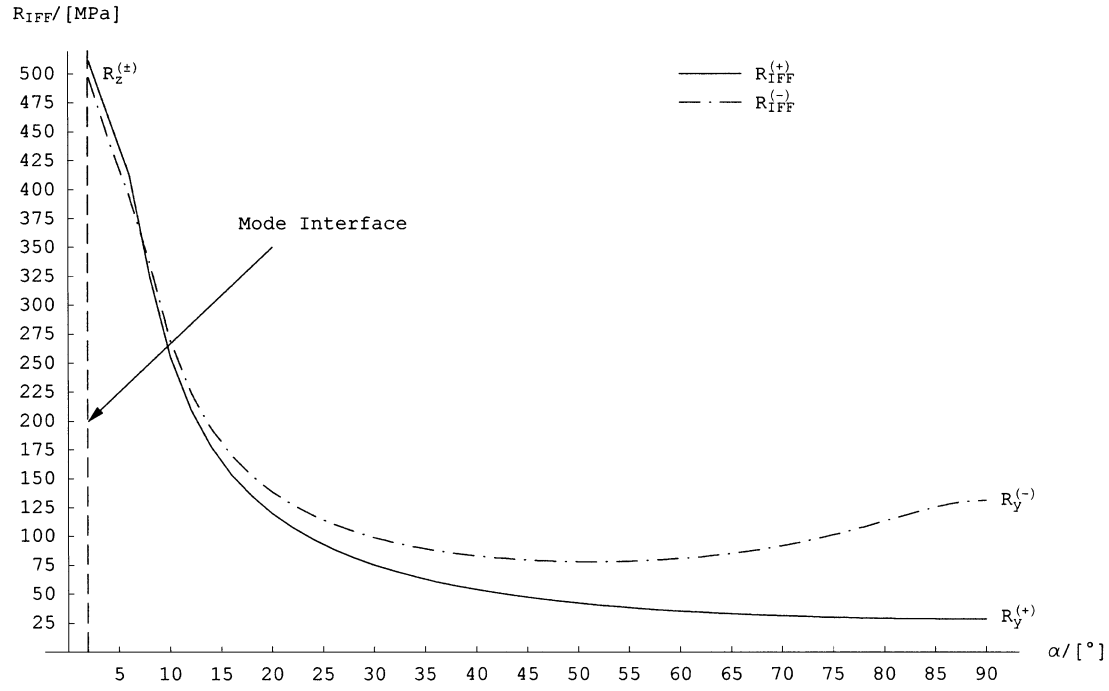

Fig. 9. Failure prediction of the SPC for off-axis loads in the y–z plane.

IFF: Eqs. (22) and (23) are used for IFF. θ Is varied from $2^\circ \leqslant \theta \leqslant 178^\circ$ compared to $0^\circ \leqslant \theta \leqslant 180^\circ$ for unidirectional layers.

6.2. Determination of material parameters

By conducting off-axis tests, normal as well as shear strength parameters for the SPC can be determined simultaneously. A direct measurement of the shear basic strengths R_{xy}, R_{xz} and R_{yz} is not necessary. All strength parameters used in the SPC are obtained by curve fitting for off-axis strength values.

6.3. Remark on the fracture angle

While it is a difficult task to measure a fracture angle for unidirectional composites in experiments, it will be almost impossible for 3D reinforced structures. The fracture angle concept has to be understood as an extremum principle. The fracture angle determines the plane where IFF will occur at first, even if a clearly defined fracture plane cannot be observed in an experiment. If the fracture hypothesis of Mohr for brittle materials is accepted as the physical basis of the PCP/SPC, then the fracture angle concept has to be accepted, too.

6.4. Remark on application for UD-compounds

The new strength model can be applied to unidirectional layers to allow for strength parameters $R_z^{(+,-)}$ smaller than $R_y^{(+,-)}$. The numerical effort is only slightly larger if the strength parameters are determined once by curve fitting.

7. Conclusion

It can be expected that laminates from unidirectional composites will remain the most commonly used kind of high performance composite structures. 3D composites will be used only where they are really necessary (e.g. in thick structures or areas where concentrated loads are applied). However, with the ongoing extension of composite application, there will be a need for 3D reinforced structures. This will cause the demand for an adequate failure criterion.

In order to meet this demand the SPC has been adapted to orthogonal 3D fiber reinforced plastics consisting of unidirectional layers with high in-plane fiber density and fiber reinforcements exactly perpendicular to the layers with a significantly lower fiber density. For composites with stronger z-reinforcements the modified criterion will yield a fracture angle $\theta = 90^\circ$ more frequently indicating that the x–z plane, the only remaining fiber parallel plane, is a preferred fracture plane. For such composites a variation of θ could not be necessary making analytical solutions of Eqs. (22) and (23) possible. That would reduce the numerical effort dramatically. The situation could then be compared with that for membrane stress states, where analytical solutions of the PCP and

SPC are known [2,5]. However, as discussed above such a configuration of 3D composites would not be reasonable.

Application of a 3D failure criterion requires to determine the complete 3D stress tensor in composites. An effective method to calculate a 3D stress state using only 2D shell elements within a finite element code was suggested by Rohwer and Rolfes [8]. This method as well as the PCP/SPC are implemented in an add-in program for MSC PATRAN named TRAVEST.

References

[1] Hashin Z. Failure criteria for unidirectional fiber composites. Journal of Applied Mechanics 1980;47:329–34.

[2] Puck A. Festigkeitsanalyse von Faser-Matrix-Laminaten: Modelle für die Praxis. München, Wien: Carl Hanser Verlag, 1996.

[3] Mohr O. Welche Umstände bedingen die Elastizitätsgrenze und den Bruch eines Materials? Z. d. VDI, 1900; Vol. 24 (45) 1524–30 and (46) 1572–77.

[4] Jeltsch-Fricker R. Bruchbedingungen vom Mohrschen Typ für transversal-isotrope Werkstoffe am Beispiel der Faser-Kunststoff-Verbunde. ZAMM 1996;76(9):505–20.

[5] Cuntze RG. et al. Neue Bruchkriterien und Festigkeitsnachweise für unidirektionale Faserkunststoffverbunde unter mehrachsiger Beanspruchung—Modellbildung und Experimente. In: Fortschrittsberichte VDI, Vol. 5, No. 506, Düsseldorf: VDI Verlag, 1997.

[6] Paluch B. Analysis of geometric imperfections affecting fibres in unidirectional composites. Journal of Composite Materials 1996; 30(4):454–85.

[7] Hashin Z, Rotem A. A fatigue failure criterion for fiber reinforced materials. Journal of Composite Materials 1973;7:448–64.

[8] Rohwer K, Rolfes R. Calculating 3D stresses in layered composite plates and shells. Mechanics of Composite Materials 1998;34: 491–500.